# Final Report: Coastal Ohio Wind Project for Reduced Barriers to Deployment of Offshore Wind Energy

**(Award Number: DE-EE0003871)**

Peter Gorsevski (Principal Investigator) [a], Abdollah Afjeh [b], Mohsin Jamali [c], Michael Carroll [d]

[a] Peter V. Gorsevski, Associate Professor, Geospatial Sciences School of Earth, Environment and Society, Bowling Green State University, Bowling Green, OH 43403-0211 (Phone: 419-372-7201; Email: peterg@bgsu.edu)

[b] Abdollah A. Afjeh, Professor, Mechanical, Industrial & Manufacturing Engineering Department, University of Toledo, Toledo, OH 43606 (Phone: 530-8210; Email: aafjeh@eng.utoledo.edu)

[c] Mohsin M. Jamali, Professor, Electrical Engineering and Computer Science Department, University of Toledo, Toledo, OH 43606 (Phone: 530-8162; Email: MOHSIN.JAMALI@utoledo.edu)

[d] Michael Carroll, Associate Professor, College of Business, Economics, Bowling Green State University, Bowling Green, OH 43403-0211 (Phone: 419-372-6053; Email: mcarrol@bgsu.edu)

**DOE Contact Information:**

Project Officer/Manager: Hahn, Michael
Phone: 720-356-1551
E-Mail: michael.hahn@go.doe.gov

Project Monitor: Carella, Michael
Phone: 720-356-1323
E-Mail: Michael.Carella@go.doe.gov

Contract Officer/Manager: Brodie, Pamela
Phone: 720-356-1449
E-Mail: pamela.brodie@go.doe.gov

Contract Specialist: Dennison, Shannon
Phone: 720-356-1315
E-Mail: shannon.dennison@go.doe.gov

Subcontractors:
University of Toledo

Project Start Date: 04/01/2011
Project End Date: 12/31/2013

**Executive Summary**

The Coastal Ohio Wind Project was created to establish the viability of wind turbines on the coastal and offshore regions of Northern Ohio. The project's main goal was to improve operational unit strategies used for environmental impact assessment of offshore turbines on lake wildlife by optimizing and fusing data from the multi-instrument surveillance system and providing an engineering analysis of potential design/operational alternatives for offshore wind turbines. The project also developed a general economic model for offshore WTG deployment to quantify potential revenue losses due to wind turbine shutdown related to ice and avian issues.

In a previous phase of this project (Award Number: DE-FG36-06GO86096), we developed a surveillance system that was used to collect different parameters such as passage rates, flight paths, flight directions, and flight altitudes of nocturnal migrating species, movements of birds and bats, and bird calls for assessing patterns and peak passage rates during migration. To derive such parameters we used thermal IR imaging cameras, acoustic recorders, and marine radar Furuno (XANK250), which was coupled with a XIR3000B digitizing card from Russell Technologies and open source radR processing software. The integration yielded a development of different computational techniques and methods, which we further developed and optimized as a combined surveillance system. To accomplish this task we implemented marine radar calibration, optimization of processing parameters, and fusion of the multi-sensor data in order to make inferences about the potential avian targets. The main goal of the data fusion from the multi-sensor environment was aimed at reduction of uncertainties while providing acceptable confidence levels with detailed information about the migration patterns.

Another component comprised of an assessment of wind resources in a near lake environment and an investigation of the effectiveness of ice coating materials to mitigate adverse effects of ice formation on wind turbine structures.  Firstly, a Zephir LiDAR system was acquired and installed at Woodlands School in Huron, Ohio, which is located near Lake Erie. Wind resource data were obtained at ten measurement heights, 200m, 150m, 100m, 80m, 60m, 40m, 38m, 30m, 20m, and 10m. The Woodlands School's wind turbine anemometer also measured the wind speed at the hub height. These data were collected for approximately one year. The hub anemometer data correlated well with the LiDAR wind speed measurements at the same height. The data also showed that on several days different power levels were recorded by the turbine at the same wind speed as indicated by the hub anemometer. The corresponding LiDAR data showed that this difference can be attributed to variability in the wind over the turbine rotor swept area, which the hub anemometer could not detect. The observation suggests that single point hub wind velocity measurements are inadequate to accurately estimate the power generated by a turbine at all times since the hub wind speed is not a good indicator of the wind speed over the turbine rotor swept area when winds are changing rapidly.

To assess the effectiveness of ice coatings to mitigate the impact of ice on turbine structures, a closed-loop icing research tunnel (IRT) was designed and constructed. By controlling the temperature, air speed, water content and liquid droplet size, the tunnel enabled consistent and repeatable ice accretion under a variety of conditions with temperatures between approximately 0°C and -20°C and wind speeds up to 40 miles per hour in the tunnel's test section. The tunnel's cooling unit maintained the tunnel temperature within ±0.2°C. The coatings evaluated in the study were Boyd Coatings Research Company's CRC6040R3, MicroPhase Coatings Inc.'s PhaseBreak TP, ESL and Flex coatings. Similar overall performance was observed in all coatings tested in that water droplets form on the test articles beginning at the stagnation region

and spreading in the downstream direction in time. When comparing ice accumulation characteristics for the four coatings tested, for ice thickness during accumulation the CRC6040R3 had the least, followed by the ESL, Flex, and TP. However, when comparing the coatings' ability to reduce ice adhesion, the Flex showed the highest adhesion reduction, followed by the ESL, TP and CRC 6040R3 coatings. The ice accumulated on the Flex coated surface shed under gravity when rotated 90 degrees following the tests while the other coatings required application of varying degrees of force to remove the ice. In conclusion, the ice coatings tested were not sufficient in preventing ice accumulation on all surfaces. However, Flex coating shows promise in mitigating ice on the rotor blades under the gravitational and centrifugal forces. Only the effect of gravity in shedding the ice was considered in this study. Further research will be needed to evaluate this coating on rotating blades in the icing tunnel to characterize its effectiveness.

Lastly, the development of economic feasibility models used existing approaches adapted for offshore deployment in marine settings to one more suitable for Lake Erie deployment. Two different wind turbine models were tested and dynamic return on investment (ROI) model scenarios were generated. For the purpose of estimating power generation three bladed wind turbines of 3 MW capacity were selected including Model1- Leitwind LTW101-3.000-kW and Model2-Vostro V90-3.0 MW. The analysis were based on the revenue aspect of decision making of deploying wind turbines in the Ohio coastal region. The installation cost, maintenance and operational aspects were disregarded due to unavailability of data. The adjusted varying price (residential and industrial sector) and projected future price of electricity in different years suggested that the Leitwind model could generate $32.4 million of revenue in 25 years if the supply electricity is in the residential sector, while it would be $14.7million if the supply is in the industrial sector. For the Vostro model these figures are $28.6 million for residential sector and $12.9 million for industrial sector for 25 years.

## Project Goals

The particular tasks of the project are:

- to improve previously developed surveillance monitoring tools that combined Radar-IR cameras and acoustic recorders for determining migratory patterns and potential impact of wind turbines across the northern shore of Lake Erie;
- to determine the effectiveness of ice coating materials and to mitigate adverse effects of ice formation on wind turbine structures; and
- to understand different economic scenarios that may emerge from deployed offshore wind turbines, suitable for Lake Erie.

## Technical Barriers

The Coastal Ohio Wind Project coordinates with the goals of the DOE Wind and Water Power Program as identified in the Wind Energy Multi-Year Program Plan for 2007-2012 by addressing key challenges to the Near- and Long-Term Vision, specifically

- Higher cost of wind energy
- Challenging regulatory and policy environment
- Increasing environmental scrutiny
- Public acceptance

## Summary of Project Accomplishments

- The marine radar surveillance system was calibrated to determine processing parameters for the radR software and other radar characteristics such as the operational beam width and the maximum range for different sizes of objects. Also, radar parameter sensitivity analyses were conducted before performing data fusion that integrated data from all three sensors including the acoustic detectors, the infrared cameras (IR), and the marine radar.

- A ZephIR LiDAR system was acquired and installed at Woodlands Intermediate School, which is located near the Lake Erie shore line. Wind resource data was collected at the school's wind turbine site for approximately one year. Wind and power data from the wind turbine were also recorded. Wind turbine and LiDAR data were compared and correlated when possible.

- Icing research studies were conducted using four commercially available coatings. An icing research tunnel was designed and constructed for this purpose. The coatings were applied to test articles that were tested in the icing research tunnel. The tests were conducted at temperatures as low as −20°C with wind speeds up to 40 miles per hour in the tunnel's test section. The icing process was recorded using a digital camera and the resulting forces were measured using a balance.

- The economic feasibility models were used to calculate the return from the investment if wind turbines were deployed in the coastal and offshore regions of Northern Ohio. For the sake of comprehensibility of the study, this component considered all technical and economic aspects of deployment.

## Specific Accomplishments

<u>Optimization of combined Radar-IR surveillance system</u>

- Calibrated the marine radar and developed different mathematical models for filtering minimum and maximum number of samples required to form blip, area of the formed blip, and angular and radial span of the formed blip

- Conducted sensitivity analysis for 10 different parameters used in radR for optimal processing of radar data

- Fusion of multi-sensor data provides the most detailed and reliable information possible. Data fusion of the radar/IR/acoustics is proposed in a hierarchical form and is based on two levels: Level 1 (L1) which is a homogenous dissimilar fusion based on feature level fusion, and Level 2 (L2) which is a heterogeneous fusion based on decision level fusion.

<u>Acquisition of Turbine Data Near Shore Environment</u>

- A ZephIR 300 LiDAR system to measure wind resource was acquired and installed at Woodlands School in Huron, Ohio. Wind resource and wind turbine operating data were obtained for one year. Wind resource data were analyzed. Data on wind shear, turbulence and wind direction were obtained.

- Woodland School's wind turbine data, power and hub wind speed, were obtained from the turbine owner. The hub wind data from the turbine anemometer was compared with the LiDAR data.

- Differences in measured data between the LiDAR device and the wind turbine anemometer were analyzed.

Studies of Icing and its Mitigation on WTG Systems

- An icing research tunnel was designed and constructed. The tunnel was equipped with force and temperature measurement sensors and data acquisition system, as well as a wireless, waterproof digital camera to capture the icing process.

- Four commercially available ice coatings were tested using a turbine rotor model (airfoil cross section) and a tower model (circular cylinder) placed in in the tunnel's test section. A water atomizer with different size nozzles was also installed in the tunnel to provide the desired droplet size and liquid water content for the tests. The nozzles' droplet size distributions were validated using TSI's laser particle image analysis system. Temperature and force data along with the videos of the icing events were recorded and analyzed.

Develop Economic Feasibility Models

- Calculated the returns from two wind turbines, both with three blades, i.e., Model1- Leitwind LTW101-3.000-kW and Model2-Vostro V90-3.0;

- Compared varying energy prices using residential and industrial sectors;

- Developed economic scenarios for new WTG operational parameters which consider icing and avian issues;

- The economic viability of both the monopole and gravity foundation designs were used in the simulation model to determine the economic consequences of each design choice.

## Project Narrative

### Overview

As the nation pushes further towards production of green energy, more and more wind turbine developments are being considered. Offshore environments are thought to be ideal places to set up wind turbines because of continuous and plentiful winds. Despite immense potential, there are no full-scale offshore wind projects that are operational or under construction in the United States. Moreover, there are no offshore wind turbines near windy, freshwater areas like the Great Lakes. The goal of the Coastal Ohio Wind Project is to establish the viability of wind turbines on the coastal and offshore regions of Northern Ohio. The project optimizes combined radar-IR surveillance system, collects and analyzes LiDAR wind data from operational wind turbine in near shore environment, conducts research on ice accretion on WTG to test various new and commercially available coatings on model test articles, and develops economic models for offshore WTG deployment to quantify potential cost savings.

## Approach

**Surveillance system.** The target detection in marine radars is difficult due to the high level of clutter and noise. The main task of the surveillance system is to identify birds and bats, which are referred to here as “targets.” The ground clutter could be reduced in the marine radar by using a protection shield around the radar beam or by elevating the antenna mount. However, various other steps in processing of marine radar data are often required for optimization and efficiency of target detection. Firstly, the marine radar was calibrated using atmospheric weather balloons with a diameter of 1.2 m filled with helium gas and capable of suspending 300 g spherical objects from hard plastic. The objects were fastened to the bottom of the balloon at specified distances while the balloons were tethered using a line from light synthetic material that extended 100 m in height. Figure 1 shows that the weather balloons were moved away from the marine radar along a transect and positional measurements of the suspended objects were taken at different distances and heights using rangefinder and Global Positioning System (GPS) receiver.

Figure 1. Marine radar calibration.

The main goal of the calibration was to determine processing parameters for the *radR* sotware and other radar characteristics such as the operational beam width  and the maximum range for different sizes of objects. Figure 2 illustrates the location of the calibration points displayed as triangles and the *radR* processing of the data.

Figure 2. Calibration data points.

The detection limits of the marine radar were explored by moving the spherical objects with the weather balloons and by measuring blips properties. The sample values which satisfy the user specified filtering conditions using *radR* are combined to form blips. Figure 3 shows Intensity decreases as a function of distance. The Intensity is the area-weighted mean intensity of the blip, from 0.0 to 1.0 where 1.0 means each sample in the blip has the maximum value possible for the radar hardware (e.g., 4095 for 12-bit digitization).

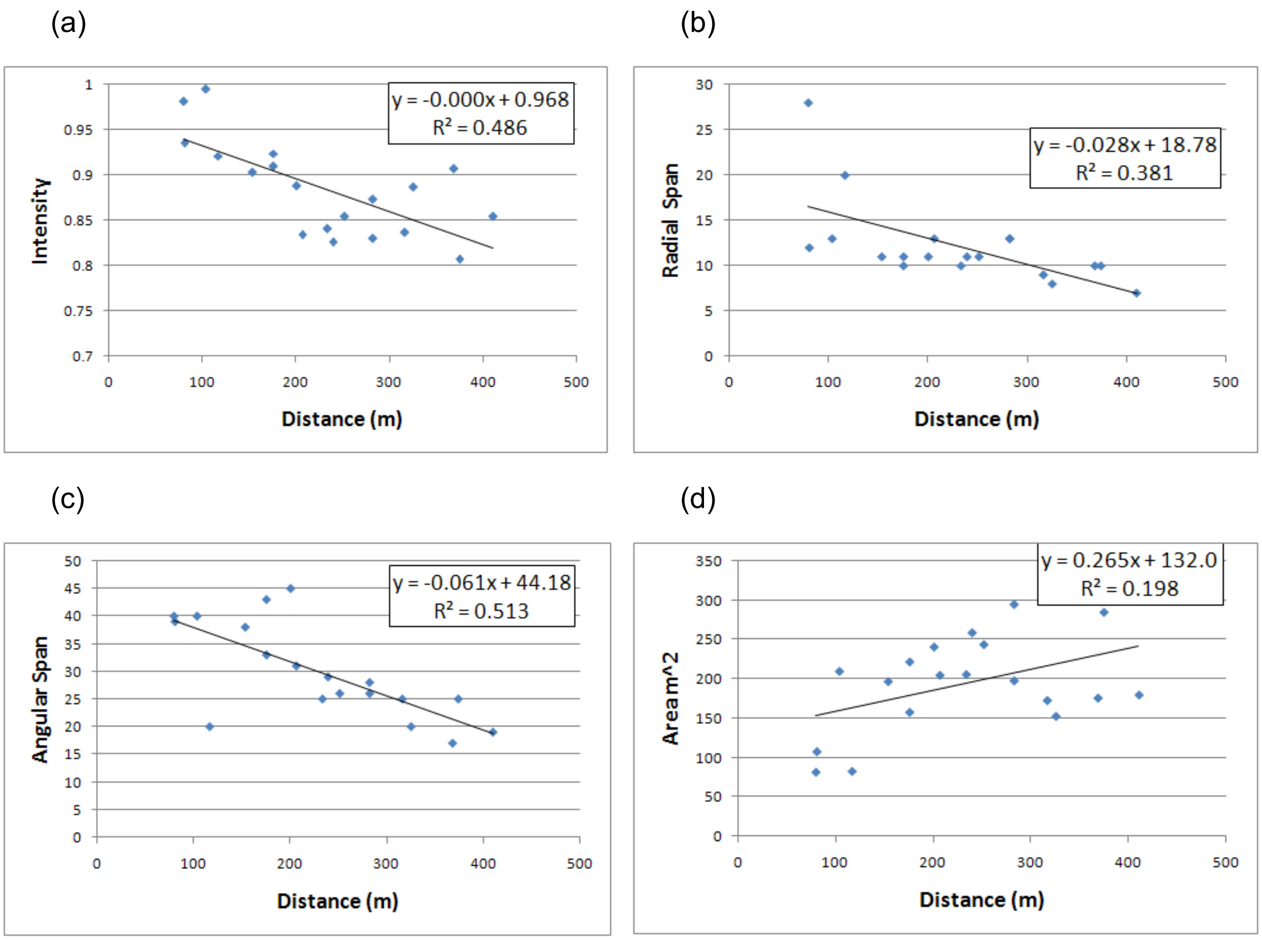


Figure 3. (a) Intensity, (b) Radial Span, (c) Angular span, and (d) Areas of the blips.

Secondly, a radar parameter sensitivity analysis was performed for applying appropriate parameters and threshold values within radR software. The results showed that some parameters have a strong impact on tracking and data analysis while other parameters may have little impact. Optimal values of these parameters for obtaining accurate results are summarized, which will be useful for wildlife biologists in developing mitigation techniques to minimize impact of wind turbines on birds and bats.

Table 1. Optimal parameter values for radar data processing

| Parameter | Min. Range | Max. Range | Optimal Value |
|---|---|---|---|
| Hot Score | 0 | 10 | 2.8 |
| Blip Ext end Diagonally | - | - | With/with out |
| Max. Speed of Tracked Object s | 0 | 200 | 100 |
| Min. Blip Area | 0 | 50000 | 300 |
| Min. Blip Sample | 2 | 50000 | 30 |
| Min. Number of Blips Required | 1 | 100 | 4 |
| Min. Gain of a Bilp in a Track | -150 | 150 | 10 |
| Number of Scans to Build Tracks | 1 | 5 | 2 |
| Number of Samples per Cell | 1 | 128 | 4 |
| Learning scans | 0 | 100 | 50 |
| Cold score | 0 | 10 | 2.5 |
| Old stats weighting | 0 | 1 | 0.95 |
| Max. blip samples | -1 | 50000 | 5000 |
| Max. blip area | 0 | 50000 | 5000 |
| Min. angular span | 0 | 1024 | 2 |
| Max. angular span | -1 | 1024 | -1 |
| Min. radial span | 0 | 1024 | 2 |
| Max. radial span | -1 | 1024 | -1 |

The last effort for optimization of the surveillance system involved a data fusion attempt that considers a multi-sensor environment of different sensor components including acoustics, infra-red (IR) camera, and marine radar. The acoustic processing component is useful for identification of avian targets by species level. The infrared sensor and IR video processing component quantifies and assigns positional x-y information to the targets.  The marine radar signal processing component assigns altitude (z- coordinates) of the target as well as other directional tracking information. The multi-sensor and multi-signal processing was used for the development of an Avian Monitoring System (AMS). In this environment, each sensor makes independent measurements and its data is processed with a unique signal processing technique. Processed data from all three sensors was used for data fusion. The AMS is shown in Figure 4 where each of the sensors provides specific information regarding these avian targets.

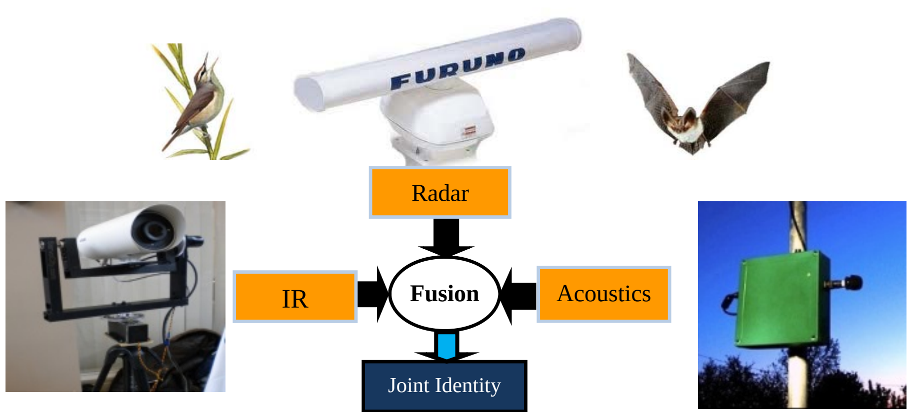


Figure 4. Multi-Sensor Multi-Signal Processing System

The acoustic processing is based on three steps: 1) data collection using acoustic detector, 2) feature extraction of the calls using different techniques such as Fast Fourier Transform (FFT), Mel Frequency Cepstrum Coefficient (MFCC), and Discrete Wavelet Transform (DWT), 3) species classification using Evolutionary Neural Network (ENN) [4], Support vector Machine (SVM), Back Propagation Neural Network (BPNN), and Discriminant Function Analysis (DFA). Figure 5 shows the block diagram of acoustic processing.

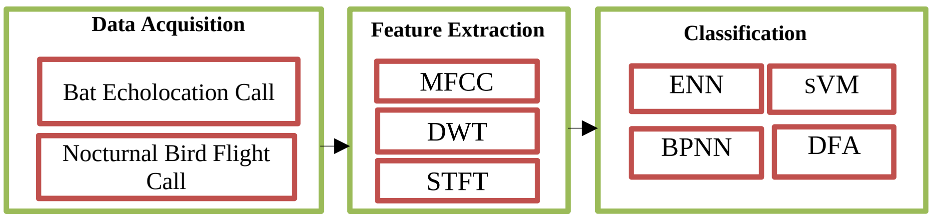


Figure 5. Acoustic Signal Processing

The IR camera provided detection and tracking of avian targets, which gives information of the flight pattern, x, y coordinates, avian target's behaviors and activity, such as direction, velocity, heat, and straightness index. The infrared images were collected using FLIR SR-19 model IR camera set up in the project area. IR processing consists of pre-processing, target detection and tracking, feature extraction, and clustering based on Fuzzy C Means (FCM) and Ant Clustering Algorithm (ACA).

Radar was used for detection and tracking of avian targets, especially in the night time and also in situations with poor visibility due to fog or clouds. Radars are also beneficial for detecting avian targets over a wider range.  Radar signal processing gives altitude information (z-coordinates) and information such as range, area, perimeter, intensity, and other statistics. A commercially available marine radar (Furuno 1500 Mark-3) is used for radar tracking. It is an X-band radar that can detect avian targets, especially in the night time and also in situations with poor visibility due to fog or clouds. Particle Filter and K-Nearest neighbor (K-NN) were used for estimation and data association, respectively.

Each sensor in AMS offers surveillance and detects the avian targets and reports it to the sensor's central processing node. The central processing node of each sensor measures the parameters (avian target signature and state parameter) and processes the decision and reports it to the fusion node. In the fusion node, the reports of all sensors are correlated and an overall decision is made. The IR and radar data are fused together based on F1 fusion node and the result will be fused with acoustics based on F2 fusion node, as shown in Figure 6. The final result is an overall inference of data from all the three sensors. Data fusion of the radar/IR/acoustics uses a hierarchical form and is based on two levels: Level 1, which is a homogenous dissimilar fusion based on feature level fusion, and Level 2, which is a heterogeneous fusion based on decision level fusion as shown in Figure 7.

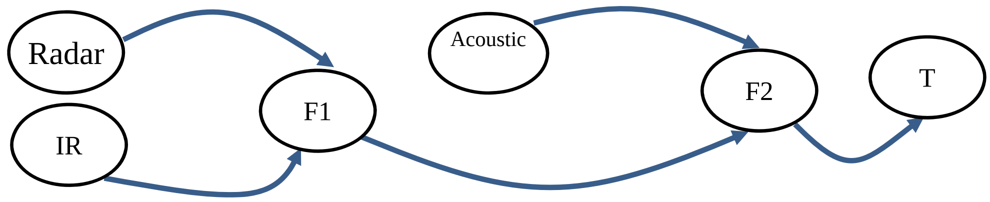


Figure 6. Fusion Process

Data fusion of IR/Radar/Acoustics involved data alignment and data association techniques. Data alignment forms a common space/time reference for fusion processing. It is divided into two main alignment operations: Spatial Alignment and Time Alignment.

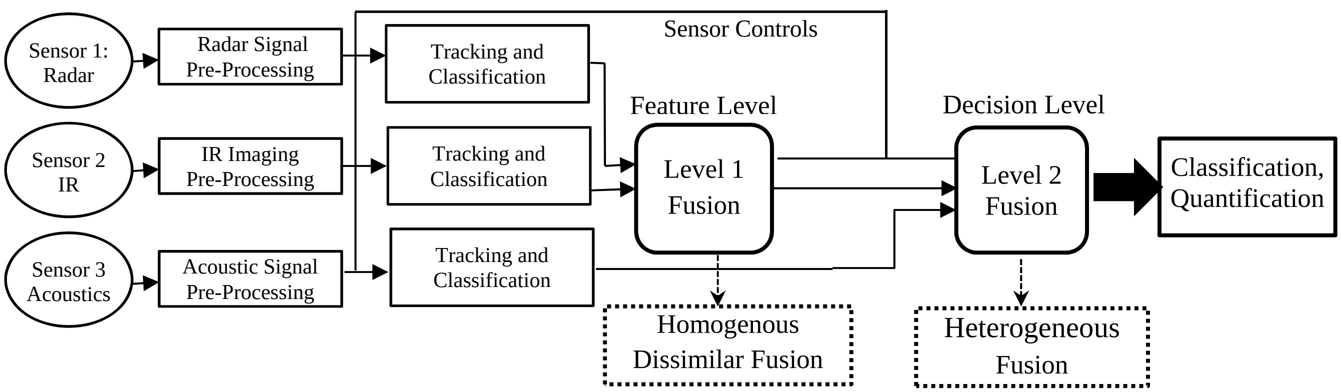


Figure 7. Data Fusion

**Acquisition of Turbine Data near Shore Environment.** In this subtask, Woodlands Intermediate School, in Huron, Ohio, was selected as the project site. The school is located approximately ¼ mile from Lake Erie shore, thus providing the needed environmental conditions for wind resource measurement. In addition, a Northern Power wind turbine is located at the school and has been providing power to the school building since March 2010. The turbine system collects wind speed, wind direction and temperature data for the operation and performance of the turbine. Power and energy production values are also recorded by the turbine operating and monitoring system. A ZephIR 300 LiDAR system was acquired for independent meteorological measurements. The ZephIR 300 uses a continuous wave technology, focusing the laser beam at the desired measurement height. The focused laser beam rotates 360 degrees, scanning to collect wind measurements in that plane. The system was first installed at the University of Toledo’s College of Engineering for evaluation and training. Campbell Scientific, the vendor, provided on-site training in February 2013. After successful evaluation of the system, the equipment was transported to the wind turbine site at Woodlands Intermediate School in Huron, Ohio, which is located approximately ¼ mile from Lake Erie. Access protocol and non-disclosure agreement (NDA) with the wind turbine owners and operators were developed and executed to gain access to the wind turbine site and operating data. Necessary utilities to power the LiDAR device were added by Woodlands School to allow its long term operation.

Figure 8. ZephIR 300 LiDAR installed beside the wind turbine tower base at Woodlands School in Huron, Ohio

Figure 9. Views of Northern Power wind turbine at Woodlands School in Huron, Ohio

**Studies of Icing and its Mitigation on WTG Systems.** This study examined passive methods of mitigating icing on wind turbine systems. This study focused on the usage of special coatings, such as ice phobic and super hydrophobic coatings, to determine the effectiveness of the coatings for wind turbine applications. Ice phobic coatings drastically reduce the adhesion force of ice, preventing ice from sticking to the surface. Super hydrophobic coatings are designed to create a very high contact angle ($\geq 150°$) between the water droplet and the surface of the object, thereby lowering the surface contact to reduce the amount of water freezing to the object. This research focused on the evaluation of these anti-icing coatings. To reproduce reliable icing conditions, an icing research tunnel (IRT) was designed and constructed at The

University of Toledo. The temperature, air speed, water content and liquid droplet size can be controlled in the IRT. The IRT's cooling system from Parameter Generation and Control (PGC) has the capacity to maintain -20 ±0.2°C using a 7500 BTU rated cooler that is powered by 230 volt, 3 phase 20 amp electric service. Therefore, the tunnel enables consistent and repeatable ice accretion under a variety of conditions with temperatures between approximately 0°C and -20°C and wind speeds up to 40 miles per hour in the tunnel's test section. Liquid particles of various sizes were introduced in the tunnel using six nozzles from Aeromist to simulate various icing conditions. The accuracy and repeatability of nozzles to produce consistently sized liquid water droplets were confirmed using the particle image technique using a pulsed laser and the TSI image processing software. The tunnel's test section is equipped with a number of strain gauges, which were used to measure wind forces and moments acting on the test articles installed in the test section. A video camera (Panasonic HX-A100D) was also installed upstream of the test section to capture the icing process on video. The camera is waterproof (up to 5 feet), has a 1080P 60 Hz full high definition (HD) video recorder, is Wi-Fi enabled, and can operate in the tunnel temperature range of interest. All sensors and the camera communicate wirelessly with a computer outside the tunnel area. National Instruments hardware and LabVIEW software were used for data collection and processing. Four commercially available ice coatings were tested during this project: one coating from Boyd Coatings Research Company, Inc. and three coatings from MicroPhase Coatings, Inc. Ice accretion on a model wind turbine rotor blade section and a model wind turbine tower was studied by measuring the tunnel temperature, water droplet size, liquid water content, wind speed and forces experienced by the models, and recording videos of the ice accretion process as a function of time.

Figure 10. Schematic overview of IRT showing Freezer unit and Observation Room

**Development of Economic Feasibility Models**. A dynamic return on investment (ROI) model that calculates the ROI at various interest rates, technologies (components) and costs was provided by the engineering design team at UT. The model specifically allowed for simulated changes in materials and costs to determine economic scenarios for new WTG operational parameters. Monte Carlo simulations were also implemented allowing for variable changes in energy prices, interest rates, and energy demand. Some of the analyses are shown below:

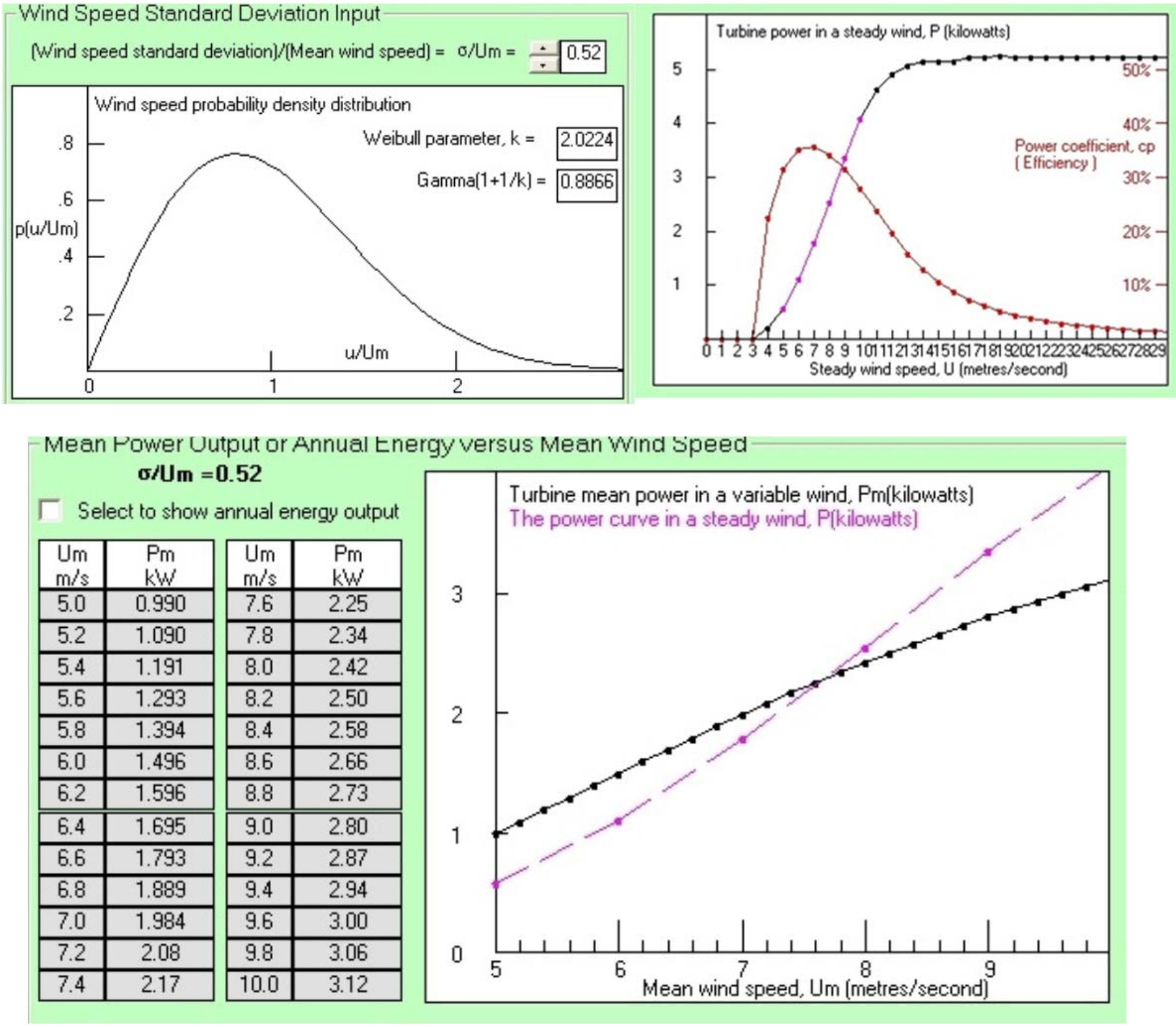


| Um m/s | Pm kW | Um m/s | Pm kW |
|---|---|---|---|
| 5.0 | 0.990 | 7.6 | 2.25 |
| 5.2 | 1.090 | 7.8 | 2.34 |
| 5.4 | 1.191 | 8.0 | 2.42 |
| 5.6 | 1.293 | 8.2 | 2.50 |
| 5.8 | 1.394 | 8.4 | 2.58 |
| 6.0 | 1.496 | 8.6 | 2.66 |
| 6.2 | 1.596 | 8.8 | 2.73 |
| 6.4 | 1.695 | 9.0 | 2.80 |
| 6.6 | 1.793 | 9.2 | 2.87 |
| 6.8 | 1.889 | 9.4 | 2.94 |
| 7.0 | 1.984 | 9.6 | 3.00 |
| 7.2 | 2.08 | 9.8 | 3.06 |
| 7.4 | 2.17 | 10.0 | 3.12 |

Figure 11. Mean Power Energy as a function of Mean Speed

Print (Total Return)/(Total Cost )    Export (Total Return)/(Total Cost) and Mean Power

**Evance Iskra R-9000 5.5m 5kw (Manufacturer's table) with wind speed standard deviation/mean speed = 0.8**

**NOTES ON CURRENCY UNITS.**

Any currency may be used for the turbine and other costs below but the reference price per kilowatt-hour must then be in units that are 1/100 of these currency units. Thus, if installation and other costs are in dollars (or euros) then the reference price per kilowatt-hour should be in cents (or euro cents). If installation and other costs are in pounds, the reference cost per kilowatt-hour should be in pence.

Turbine cost = 25,000 *Essential    Installation and other fixed costs = 2,000 *Non-essential    Annual recurrent costs = 250 *Non-essential

Reset    Calculate (Total Return)/(Total Cost)

Wind turbine life (5 to 50 years) = 20    Reference price per kilowatt-hour (range 1 to 99.9) = 33 . 7

| U m/s | Return (Total cost) | Equiv. interest (%) | U m/s | Return (Total cost) | Equiv. interest (%) |
|---|---|---|---|---|---|
| 5.0 | 2.10 | 3.79 | 7.6 | 3.71 | 6.77 |
| 5.2 | 2.25 | 4.13 | 7.8 | 3.81 | 6.91 |
| 5.4 | 2.39 | 4.44 | 8.0 | 3.90 | 7.04 |
| 5.6 | 2.52 | 4.74 | 8.2 | 3.99 | 7.16 |
| 5.8 | 2.66 | 5.01 | 8.4 | 4.08 | 7.28 |
| 6.0 | 2.79 | 5.26 | 8.6 | 4.16 | 7.39 |
| 6.2 | 2.92 | 5.50 | 8.8 | 4.24 | 7.49 |
| 6.4 | 3.04 | 5.72 | 9.0 | 4.31 | 7.58 |
| 6.6 | 3.16 | 5.92 | 9.2 | 4.38 | 7.67 |
| 6.8 | 3.28 | 6.12 | 9.4 | 4.45 | 7.75 |
| 7.0 | 3.39 | 6.30 | 9.6 | 4.52 | 7.83 |
| 7.2 | 3.50 | 6.47 | 9.8 | 4.58 | 7.90 |
| 7.4 | 3.61 | 6.62 | 10.0 | 4.64 | 7.97 |

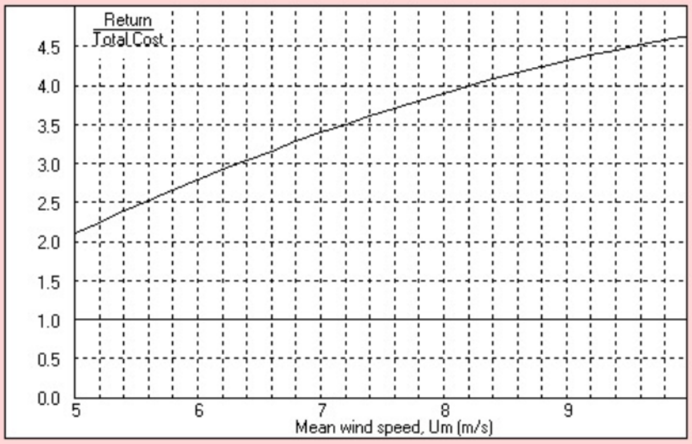


**Evance Iskra R-9000 5.5m 5kw (Manufacturer's table) with wind speed standard deviation/mean speed = 0.8**

**NOTES ON CURRENCY UNITS.**

Any currency may be used for the turbine and other costs below but the reference price per kilowatt-hour must then be in units that are 1/100 of these currency units. Thus, if installation and other costs are in dollars (or euros) then the reference price per kilowatt-hour should be in cents (or euro cents). If installation and other costs are in pounds, the reference cost per kilowatt-hour should be in pence.

Turbine cost = 25,000 *Essential    Installation and other fixed costs = 2,000 *Non-essential    Annual recurrent costs = 250 *Non-essential

Reset    Calculate payback period (years)

Reference price per kilowatt-hour (range 1 to 99.9) = 33 . 3

| U m/s | Payback (years) | Annual income | U m/s | Payback (years) | Annual income |
|---|---|---|---|---|---|
| 5.0 | 8.78 | 3,327 | 7.6 | 4.81 | 5,864 |
| 5.2 | 8.18 | 3,551 | 7.8 | 4.68 | 6,018 |
| 5.4 | 7.67 | 3,772 | 8.0 | 4.56 | 6,167 |
| 5.6 | 7.22 | 3,989 | 8.2 | 4.46 | 6,309 |
| 5.8 | 6.83 | 4,201 | 8.4 | 4.36 | 6,446 |
| 6.0 | 6.49 | 4,409 | 8.6 | 4.27 | 6,576 |
| 6.2 | 6.19 | 4,611 | 8.8 | 4.19 | 6,701 |
| 6.4 | 5.92 | 4,807 | 9.0 | 4.11 | 6,820 |
| 6.6 | 5.69 | 4,998 | 9.2 | 4.04 | 6,933 |
| 6.8 | 5.47 | 5,183 | 9.4 | 3.98 | 7,040 |
| 7.0 | 5.28 | 5,363 | 9.6 | 3.92 | 7,142 |
| 7.2 | 5.11 | 5,536 | 9.8 | 3.86 | 7,239 |
| 7.4 | 4.95 | 5,703 | 10.0 | 3.81 | 7,331 |

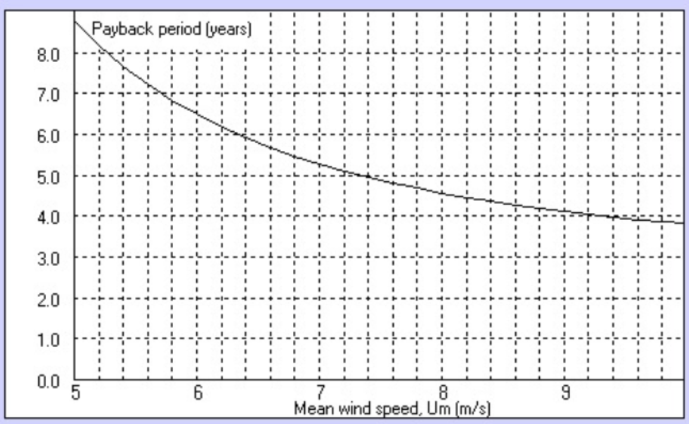


Annual income is the annual kW-hrs generated

Figure 12. Total return and payback period

## Results

**Surveillance system**. The data fusion results were generated from spring and fall 2011 migration in the western basin of Lake Erie in Ohio. The number of passes for two bird classes (Thrush and Sparrow) and bat species (Labo and Epfu) for the fall 2011 migration period in Toledo and ONWR are shown in Figure 13.

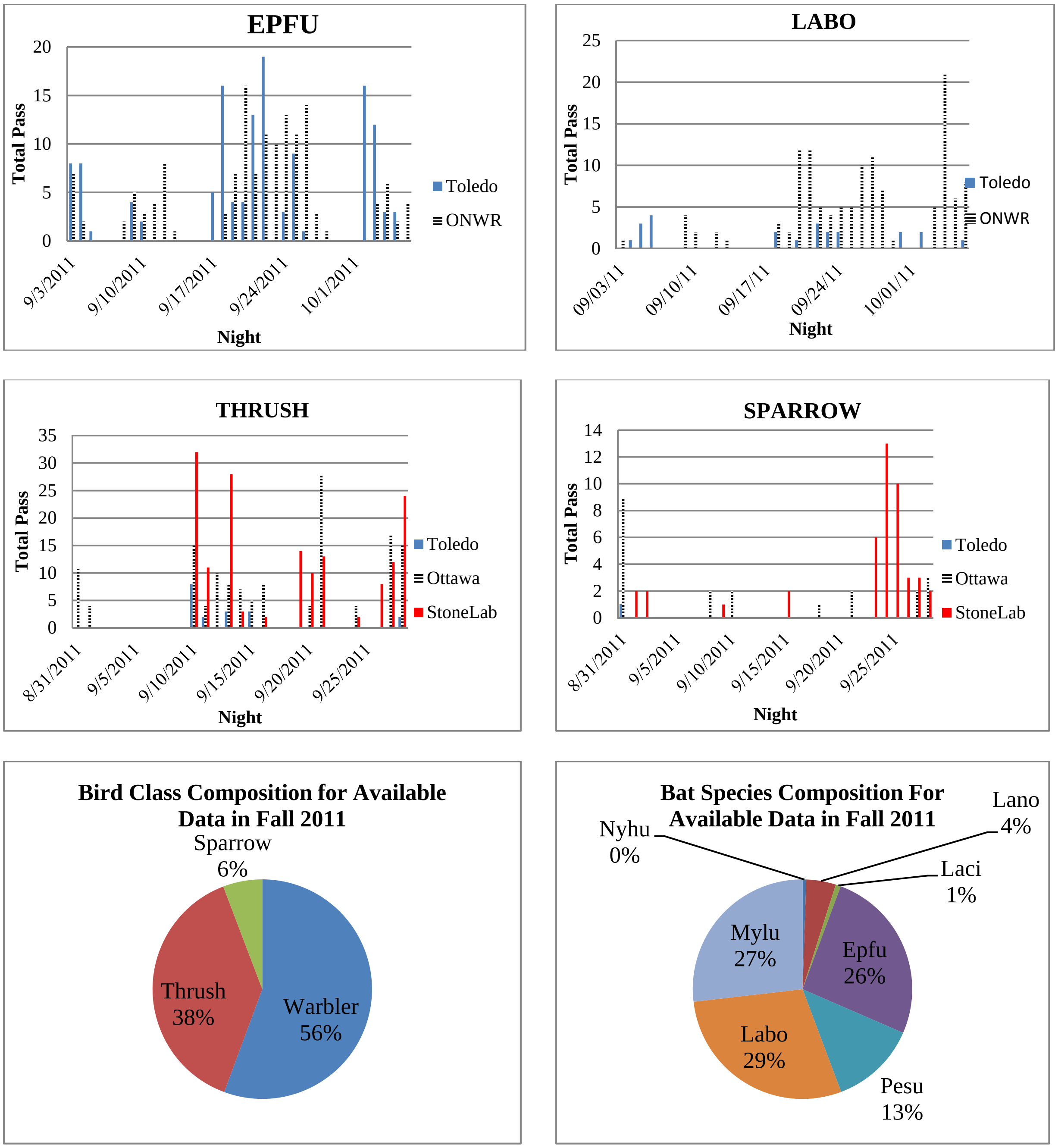


Figure 13. Bird classes and composition from data fusion.

Overall bird class composition in ONWR in fall 2011 are shown in Figure 13. It can be seen that Warblers with 56% of all flight calls contain the majority of the bird classes. The figure also shows the overall bat species composition in ONWR in fall 2011. The total number of bird flight calls and bat echolocation calls in spring 2011 are shown in Figure 14.

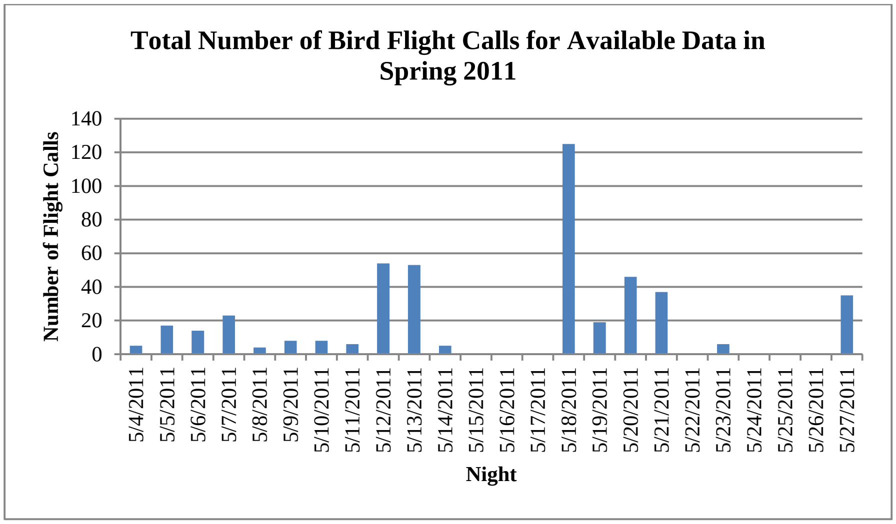


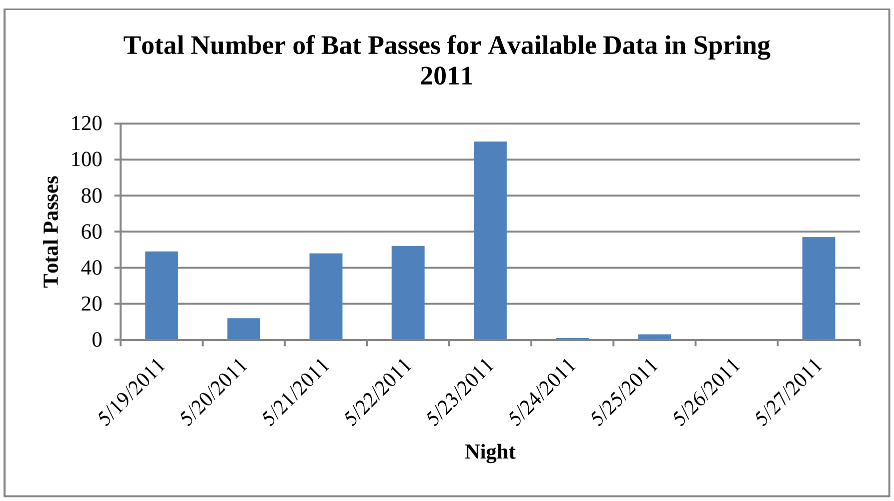


Figure 14. Total number of bird flight calls and bat passes

**Acquisition of Turbine Data near Shore Environment .** The ZephIR Lidar measures the wind speed at 10 different heights. This information was used to determine the wind velocity profile. Examples of these data are shown in Figures 14 - 16. Figure 14 shows an example of the Lidar data for selected heights 40m, 60m, and 80m. The wind speed as measured by the wind turbine hub anemometer is also included in the graph for comparison. The data clearly shows the dependence of the wind speed on elevation. Hence, hub height wind speed value may not be an accurate measure of wind speed to optimally capture the wind energy.

This observation can be confirmed by considering the turbine actual power. Figure 15 shows the actual power measured at a given time by the turbine's control system. Superimposed on the data is the computed available wind power $(\frac{1}{2}\rho AV^3)$ using the measured hub wind speed.

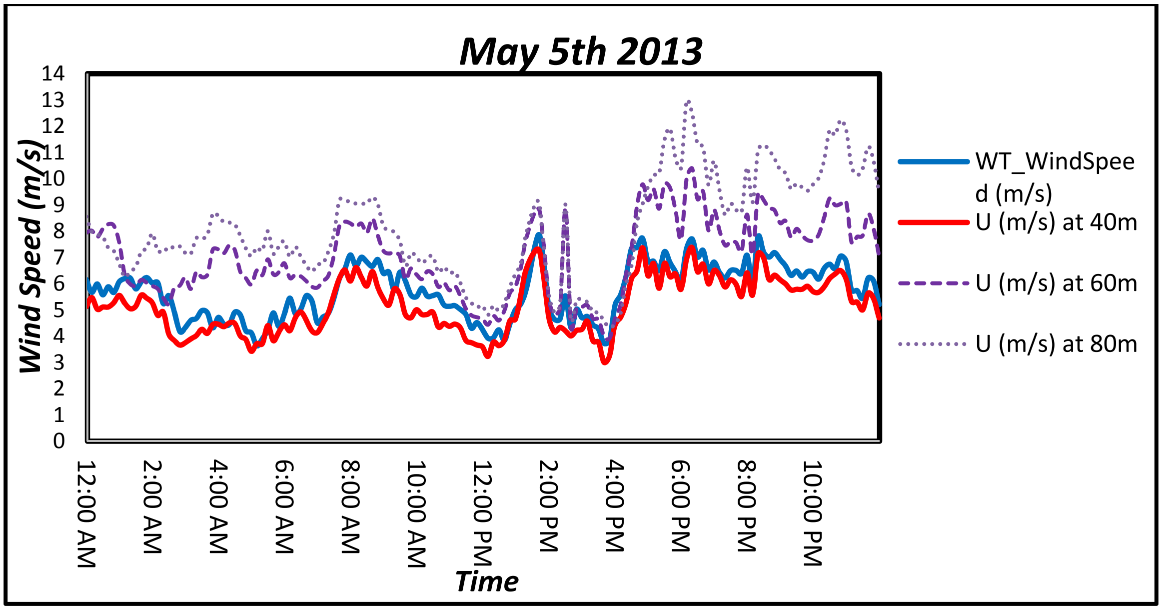


Figure 14. Comparison of LiDAR wind speed data at 40m, 60m, and 80m elevations with the wind turbine hub anemometer data at height 40 m, 60 m, and 80 m.

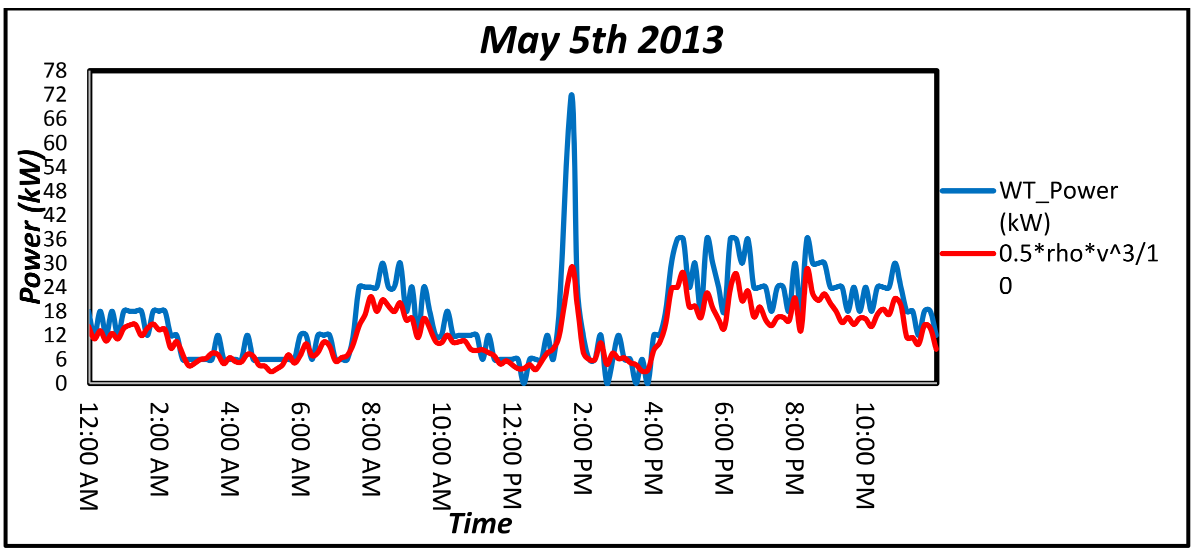


Figure 15. Comparison between turbine output power of available wind power ($0.5 * \rho * V^3/10$) on May 5th 2013

Furthermore, the data show that a change in height of 20 m from 40 m to 60 m increases the wind speed considerably more than the exact change in height from 60 m to 80 m. Therefore, the most cost effective choice for the wind turbine height requires accurate knowledge of the site's wind characteristics.

The wind turbine hub height is approximately 40 m; therefore, the Lidar wind speed data at 40 m corresponds to those recorded by the wind turbine's hub anemometer.  Figure 14 shows that the LiDAR anemometer data compare well, validating proper operation of both the anemometer and Lidar devices. Data for other days confirmed that LiDAR and anemometer data compared well at the hub height. The wind profile is also measured by LiDAR. Figures 15 and 16 display two examples of the wind profile, showing that the wind profile can be quite complex and may not be adequately described by a single wind shear parameter.

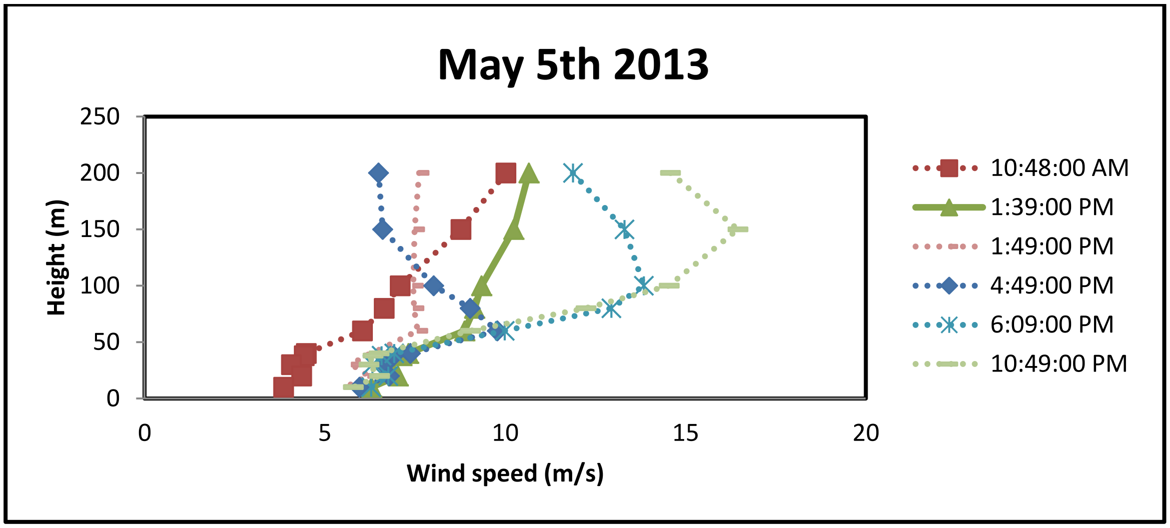


Figure 16. Wind profiles for different times on May 5th 2013.

Turbulence intensity was also measured at the Woodlands Schools site. Figure 17 shows an example. Measured turbulence intensity decreases substantially with increasing height. The measurements over time document a quantitative estimate of this reduction.

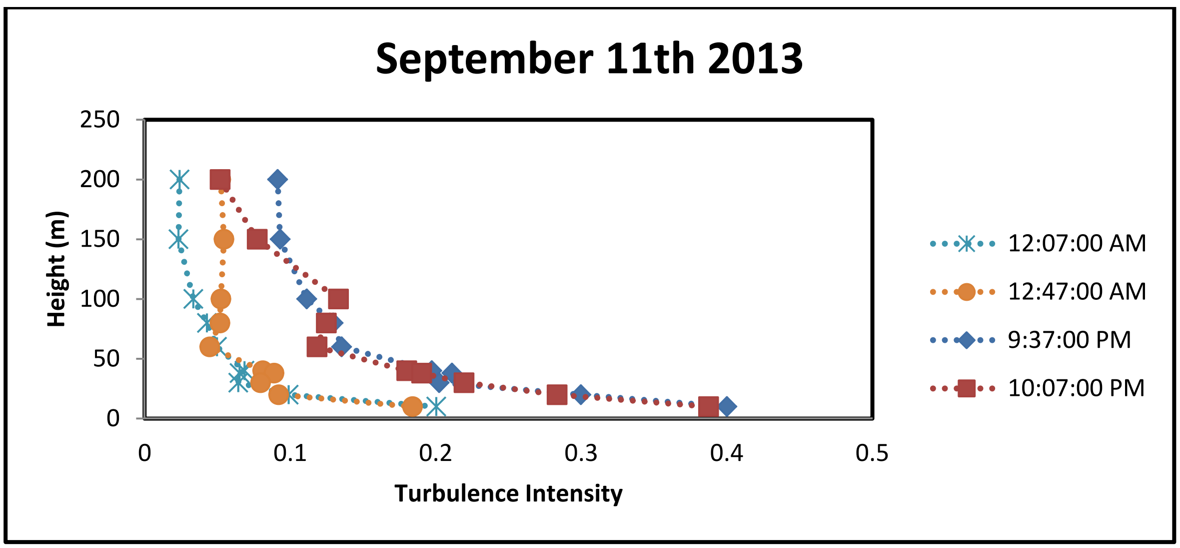


Figure 17. Turbulence intensity variations with height for different times on May 5th 2013.

**Studies of Icing and its Mitigation on WTG Systems.** An icing research tunnel was constructed. The tunnel's test section is equipped with a thermocouple, a pressure transducer, and a number of strain gauges, which were used to measure wind forces and moments acting on the test articles installed in the test section. A video camera (Panasonic HX-A100D) installed inside the tunnel recorded video images of the icing process. Four commercially available coatings were used in the tests: Boyd Coatings Research Company CRC6040R3, and MicroPhase Coatings Inc. PhaseBreak TP, ESL and Flex coatings. Figures 18 -20 show the test article icing treated with the CRC6040R3 coating.

Figure 18. Leading Edge Ice Formation on Airfoil Treated with CRC6040R3

Figure 19. Trailing Edge View Ice Formation on Airfoil Treated with CRC6040R3

Figure 20. Side View of Leading Edge Ice Formation on Airfoil Treated with CRC6040R3

The view of ice formation on the leading edge of the test article treated with PhaseBreak TP is shown in Figure 21. Although glaze ice is forming icicles on the leading edge, the characteristic of the ice on this surface is different, exhibiting individual droplet icing structures, as can be seen on the upper side of the airfoil shown in Figure 22.

Figure 21. Leading Edge Ice Formation on Airfoil Treated with PhaseBreak TP

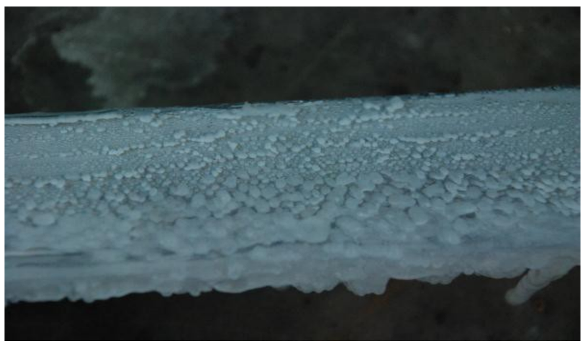

Figure 22. After Icing Test Results – Zoomed in View of Upper Surface

Examples of the PhaseBreak ESL results are shown in Figure 23. Ice formed on the leading edge during the tests, but the ESL coating resulted in droplet icing structures more defined than were visible with the TP coating on the airfoil's upper surface and the leading edge, forming fewer but thicker icicles, as Figure 23 depicts. Also, the ESL coating had a lower ice adhesion than the TP, requiring only a soft touch to shed the ice from the surface.

Figure 23. Leading Edge Ice Formation on Airfoil Treated with PhaseBreak ESL

To study the effect of wind speed on ice formation, the tunnel wind speed was varied form 11.9 m/s to 16.8 m/s (25.7 mph to 37.6 mph). The test was run for 5 minutes to study the progression of ice formation on the surface.

- **CRC6040R3 Coating.** A photograph of the airfoil treated with this coating is shown in Figure 24. The tests were conducted for 5 minutes at different speeds of at 11.9 m/s (25.7 mph) and 16.8 m/s (37.6 mph). Ice formed on the leading edge and the two ends of the section, but liquid water remained in the middle section and continued to shed over the trailing edge. As expected, the ice thickness where formed was considerably smaller at high speeds compared with the low speed tests. The ice was removed with some force at the end of the tests.

- **PhaseBreak Flex Coating**. Similar to the CRC6040R3 coating, the test at the lower speed produced thicker ice than the test at the higher speed. Icicles were present only at the lower speed. Also, the ice accretion on the surface for this coating was thicker that the ice formation grown on the CRC6040R3, as can be seen in Figure 25. Unlike the CRC6040R3 coating, however, the ice was removed easily under gravity when the blade was rotated 90 degrees.

(a) Wind speed 11.9 m/s (25.7 mph)

(b) Wind speed 16.8 m/s (37.6 mph)

Figure 24. Leading Edge Ice Formation on Airfoil Treated with CRC6040R3

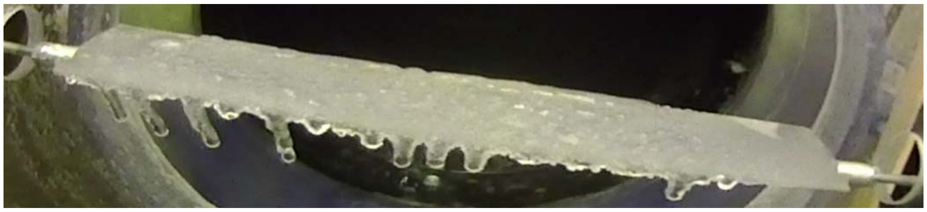

(a) Wind speed 11.9 m/s (25.7 mph)

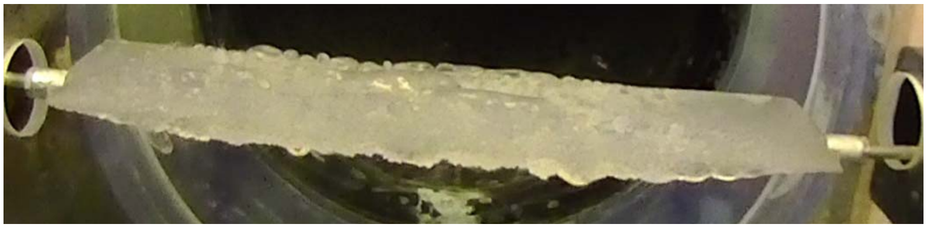

1. Wind speed 16.8 m/s (37.6 mph)

Figure 25. Leading Edge Ice Formation on Airfoil Treated with PhaseBreak Flex

- **PhaseBreak TP Coating.** The ice accretion for this coating was very similar to that of PhaseBreak Flex coating. But application of a force was required to remove the ice.
- **PhaseBreak ESL Coating**. The ice accretion for this coating was similar to the CRC6040R3 coating in that the ice accumulation remained relatively thin, a large portion of the blade continually shed liquid water from the trailing edge, and a substantial portion of the blade remained ice free. The removal of the ice required some force although smaller than the TP. Thus ESL was different than the CRC6040R3 coating where any accreted ice shed easily with a soft touch without requiring any additional force. Figure 2.9 shows the results for this coating.

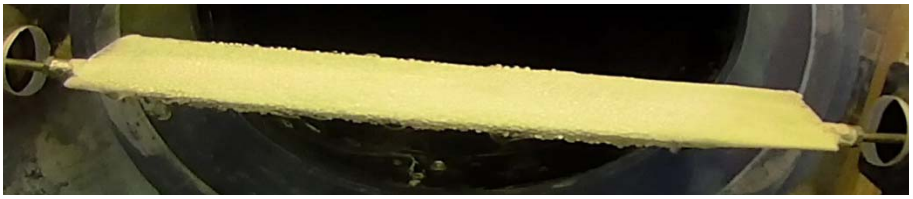

(a) Wind speed 11.9 m/s (25.7 mph)

(b) Wind speed 16.8 m/s (37.6 mph)

Figure 26. Leading Edge Ice Formation on Airfoil Treated with PhaseBreak ESL

**Economic Feasibility Model.** The adjusted varying price (residential and industrial sector) and projected future price of electricity in different years suggested that the Leitwind model will generate $32.4 million of revenue in 25 years if the supply electricity is in the residential sector while $14.7million if the supply is in the industrial sector.

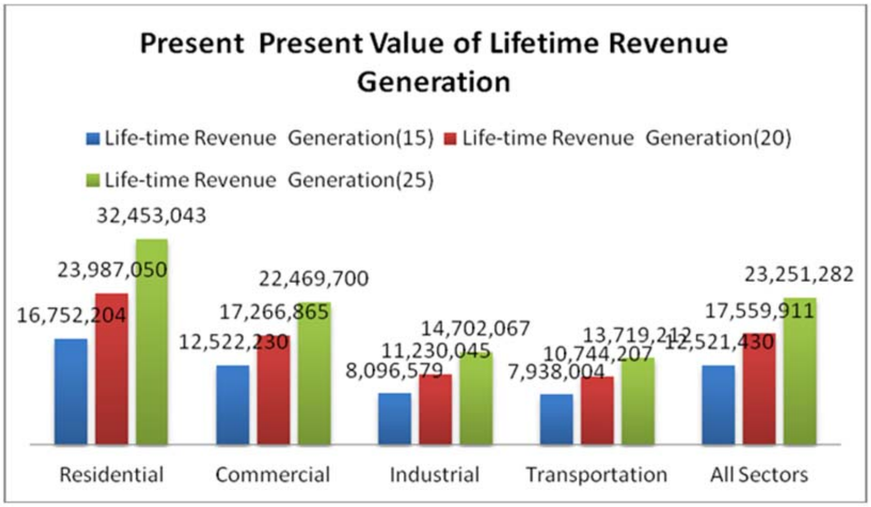


Figure 27. Total Present Value of Life-time Revenue Generation (Leitwind)

Lifetime revenue generation was also considered by including icing and avian issues in the ROI model. Some of the difficulties were associated with the uncertainties of icing data on the precise number of days in which an average severe ice fall occurs, with the exact timing of seasonal bird migration, which leads to a complete shutdown. Therefore our assumption was to designate a sound approximation that 15 days in January the wind turbine may shut down completely due to severe icing (of course if severe icing is not experienced in a particular year, the wind turbine would then be full in operation). To remove the barrier and reduce the probability of killing birds during the season of migration we used the likelihood that one week of April (spring) and one week of October (fall) the wind turbine may remain shut down depending on the local experience of bird migration. Figure 28 shows that life-time revenue generation (25 years) ranges between $10.1 million for industrial and $19.2 million for residential. The life-time revenue generation (25 years) for all sectors is expected to be $15.2 million.

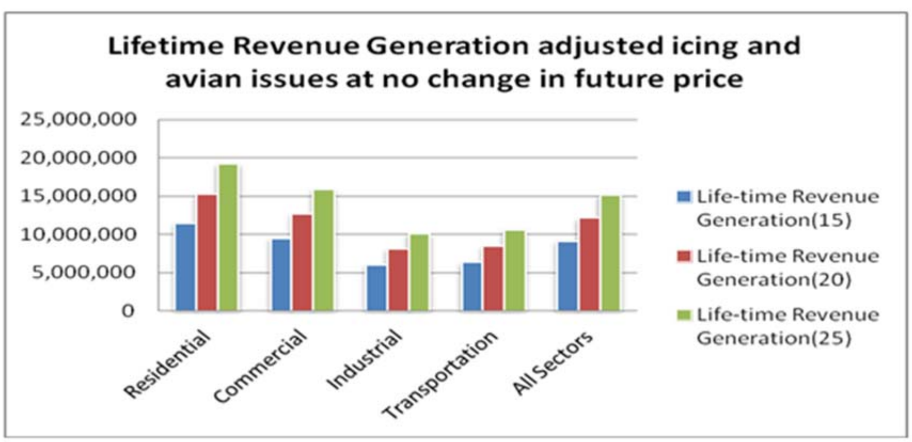


Figure 28. Lifetime Revenue Generation adjusted for icing and avian issues at no change in future price (Leitwind Model)

In addition, thirty years of wind data was collected and analyzed to determine the efficiency of proposed wind farm. If we assume that price will be constant and future income is equivalent to current income then total lifetime revenue generation will be as follows. Table 2 below shows income after adjusting from avian and icing issues (table calculated on constant price).

Table 2. Total Revenue after adjusted for avian and icing issues and with no price change and no discounting

| | Residential | Commercial | Industrial | Transportation | All Sectors |
|---|---|---|---|---|---|
| Life-time Revenue Generation(15) | 10,198,110 | 8,456,309 | 5,360,419 | 5,649,573 | 8,366,658 |
| Life-time Revenue Generation(20) | 13,597,480 | 11,275,079 | 7,147,225 | 7,532,763 | 11,155,545 |
| Life-time Revenue Generation(25) | 16,996,850 | 14,093,849 | 8,934,031 | 9,415,954 | 13,944,431 |

Since the expected revenue generation for the proposed wind turbine will occur in future years, the predicted revenue generation was adjusted with the future price. Figure 29 shows variation of the Monthly Retail Price of electricity from October 2002 to April 2013 from EIA database used in Table 3 for different categories of end use.

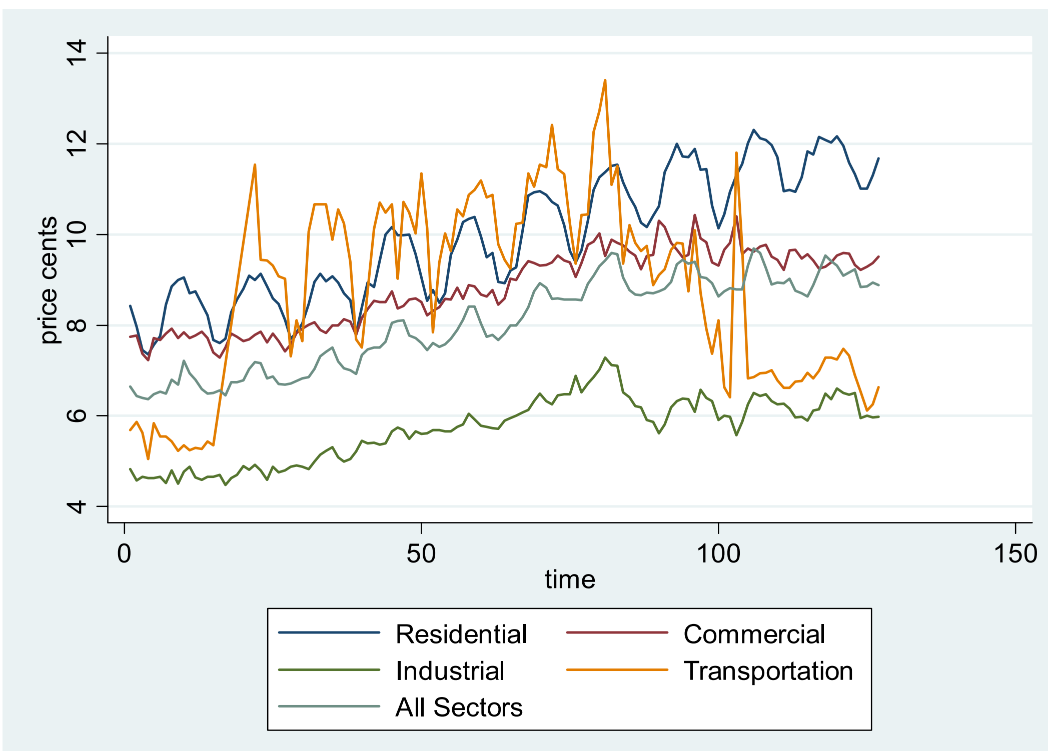


Figure 29. Variation of Retail Electricity Price from 2002 to 2013

By considering the future price as well as changed discount rate in future years and using the present value of the future return of a Leitwind LTW101-3.000-kW wind turbine is shown in the following Table 3. The table suggests the life-time revenue generation (25 years) for all sectors is expected to be $20.5 million.

Table 3. Total Revenue Generation after adjusting icing and avian issues at varied price and discounting

| | Residential | Commercial | Industrial | Transportation | All Sectors |
|---|---|---|---|---|---|
| Life-time Revenue Generation(15) | 14,827,259 | 11,083,339 | 7,166,226 | 7,025,872 | 11,082,631 |
| Life-time Revenue Generation(20) | 21,230,771 | 15,282,783 | 9,939,635 | 9,509,623 | 15,542,155 |
| Life-time Revenue Generation(25) | 28,723,963 | 19,887,776 | 13,012,697 | 12,142,779 | 20,579,548 |

The total loss for the Leitwind model due to shut down using adjusted varying price is shown in Table 4.

Table 4. Total loss projection in Leitwind model due to avian and icing issues

| | Residential | Commercial | Industrial | Transportation | All Sectors |
|---|---|---|---|---|---|
| Life-time Revenue Generation(15) | 1,924,945 | 1,438,891 | 930,353 | 912,132 | 1,438,799 |
| Life-time Revenue Generation(20) | 2,756,279 | 1,984,082 | 1,290,410 | 1,234,584 | 2,017,756 |
| Life-time Revenue Generation(25) | 3,729,080 | 2,581,924 | 1,689,370 | 1,576,433 | 2,671,734 |

## Conclusions and Future Directions

In this study, the optimization of the surveillance system involved calibration of the marine radar, optimization of parameters used to extract blips from the marine radar, and data fusion that considered integration of multi-sensor environment using three different sensors: acoustics, infrared camera (IR), and radar for the development of an Avian Monitoring System (AMS). The data fusion approach implemented different signal processing techniques including pattern recognition, machine learning, signal processing, bio-inspired computing, probabilistic methods, and fuzzy reasoning. The aim of this approach was to reduce uncertainties and provide information about the patterns with the desired level of confidence using different sensing properties. For example, the acoustic processing component identifies avian targets by species level, the infrared sensor and IR video processing component quantifies and assigns positional x-y information to the targets, and the marine radar signal-processing component assigns altitude (z- coordinates) of the target as well as other directional tracking information.
The data fusion, which was done so as to reduce uncertainties with the quantification of avian targets, was implemented in the western basin of Lake Erie in Ohio using surveillance data from spring and fall 2011 migration time. Our previous project (Award Number: DE-FG36-06GO86096) describes the inferences from the surveillance data.

Although the results are promising further research is needed to better quantify accuracy assessment with this optimization approach. For instance, thorough calibration of thermal cameras and acoustic equipment, field groundtruthing, validation and integration with other monitoring tools designed for different spatial scales such as NEXRAD can improve the accuracy of avian targets.

Furthermore, a LiDAR system was acquired and installed at Woodlands School site, less than ¼ mile from the Lake Erie shore line. Wind resource data and power from the Northern Power wind turbine at the site were recorded for approximately one year. Wind speed and direction were also measured at the turbine's hub height using the turbine's anemometer. LiDAR data at the same height as the wind turbine anemometer matched favorably with the anemometer data. It was observed that the wind speed changed significantly over the turbine swept area during some days and that a single wind speed measurement at the hub height was inadequate to predict the available wind power. Specifically, different power levels were produced by the wind turbine at the same wind speed recorded by the anemometer. However, the LiDAR data showed that the wind speed over the turbine swept area was drastically different for the identical hub wind speeds. Using LiDAR data, the potential for power production at a given site can be more reliably predicted, thus reducing the investment risk in the selection of a wind farm site. Future research should be conducted to collect wind and power data over a longer period of time to develop and validate models to predict wind turbine power from wind measurements over the entire wind turbine swept area.

An icing research tunnel was designed and constructed to study the effectiveness of ice coatings in preventing ice formation on wind turbine structures. Four commercially available ice coatings were tested in the tunnel at different speeds and a range of temperatures. It was found that the coatings behaved differently. Two general categories of ice accumulation were observed. Thick ice formed on the MicroPhase PhaseBreak Flex and PhaseBreak TP coatings. Thin ice was formed on Boyd CRC6040R3 and PhaseBreak ESL coatings. The CRC6040R3 had the least thickness, followed by the ESL, Flex, and TP. When comparing the coating's ability to reduce ice adhesion, the Flex showed the highest adhesion reduction, followed by the ESL, TP and CRC 6040R3 coatings. With the Flex coating, the ice was able to shed by gravitational force only, while the others required varying degrees of additional force. During the high speed tests, thinner ice formed along the leading edge and more liquid water was shed from the trailing edge over the surface of the airfoil regardless of the kind of coatings. When considering the four coatings for wind turbine applications, the choice of the coating should depend on the turbine site, for example, how much ice can accumulate and how easily is the ice shed. If a wind turbine is located in a remote region, shedding ice is not a concern and a coating with the least adhesion can be used. Future research can be conducted to evaluate the coatings ability to mitigate ice on rotating blades. The presence of centrifugal forces on rotating structures introduces a body force in addition to the force of gravity that may help accelerate liquid droplets to travel to the trailing edge of the blade and facilitate shedding ice from the surface. Such a test can be done in the existing icing tunnel using a rotary test stand.

The economic feasibility model presented different scenarios of calculating returns using two different wind turbine models (Model1- Leitwind LTW101-3.000-kW and Model2-Vostro V90-3.0 MW). The simulation with varying electricity retail prices suggested that the Leitwind model will generate $32.4 million of revenue in 25 years if they supply electricity in the residential sector and $14.7million if they supply it in the industrial sector. For the Vostro model these figures are $28.6 million for the residential sector and $12.9 million for the industrial sector for 25 years. However, the total loss due to assumed shut down suggested that the Leitwind model would lose $3.7 from the residential sector and $1.7 from the industrial sector. The losses from the Vostro model are slightly less, where $3.1 is from the residential and $1.4 from the industrial sector. However, one of the challenges for the development of offshore wind turbine economic scenarios in the Great Lakes region is the lack of distributed spatio-temporal data across the lake, which could significantly improve the economic feasibility predictions.

**Publications/Presentations**

Whitacre, David Lewis, “Development of an Icing Research Wind Tunnel at The University of Toledo,” MS Thesis, December 2013.

Qiuying Zhao, Jacob Ickes, Chunhua Sheng, and Abdollah Afjeh, “Numerical Investigation of Upwind and Downwind NREL 5MW Reference Wind Turbines,” Accepted for presentation at AHS 70th Annual Forum, May 2014.

Jin Woo Lee, Efstratios Nikolaidis, and Abdollah Afjeh, “Efficient Stress Estimation Method for Dynamic Wind Turbine Simulation Using FAST Results,” AWEA Offshore Windpower Conference and Exhibition, Providence, Rhode Island, Oct. 2013.

Amin Jarrah, Mohsin M. Jamali, Jeremy Ross, Peter V. Gorsevski, Joseph Frizado, Verner P. Bingman, “Sensitivity Analysis for Optimal Parameters for Marine Radar Data processing,” American Journal of Signal Processing, Volume 3, Number 3, August 2013. p-ISSN: 2165-9354 e-ISSN: 2165-9362, 2013; 3(3): 78-83, doi:10.5923/j.ajsp.20130303.05, (http://article.sapub.org/10.5923.j.ajsp.20130303.05.html)

Golrokh Mirzaei, Mohammad Wadood Majid, Jeremy Ross, Mohsin M. Jamali, Peter V. Gorsevski, Joseph Frizado,Verner P. Bingman, “Acoustic/IR Monitoring via Machine Learning,” Submitted to International Journal of Hybrid Intelligent systems.

Golrokh Mirzaei, Selin Bastas, Mohsin M. Jamali, Mohammad Wadood Majid, Peter V. Gorsevski, Verner P. Bingman,” Avian Call Recognition System,” Submitted to the IEEE Transactions on Signal Processing.

G. Mirzaei, M. W. Majid, M. M. Jamali, J. Ross, J. Frizado, P. V. Gorsevski, V. Bingman, “ The Application of Evolutionary Neural Network for Bat Echolocation Calls Recognition,” Paper presented at 2011 International Joint Conference on Neural Networks

M. M. Jamali, Brett Snyder, John Williams, Ryan Kindred, Gavin St. John, M. W. Majid J. Ross, J. Frizado, P. V. Gorsevski, V. Bingman, “Radar/IR Based Avian Monitoring System for Wind Turbines,” Poster presented at the 2011 The University Clean Energy Alliance of Ohio Annual Conference, April 2011.

G. Mirzaei, M. W. Majid, S. Bastas, M. M. Jamali, J. Ross, J. Frizado, P. V. Gorsevski, V. Bingman, “Bio-acoustic Monitoring of Birds/Bats in the vicinity of Wind Turbines,” Poster presented at the 2011 The University Clean Energy Alliance of Ohio Annual Conference, April 2011.

G. Mirzaei, M. W. Majid, S. Bastas, M. M. Jamali, J. Ross, J. Frizado, P. V. Gorsevski, V. Bingman," The Bio-Acoustic Feature Extraction of Bat Echolocation Calls," paper submitted to the 2012 IEEE International Conference on Electro/Information Technology, May 2011.

G. Mirzaei, M. W. Majid, J. Ross, M. M. Jamali, J. Frizado, P. V. Gorsevski, V. Bingman, " Avian Detectopm & Tracking Algorithm Using Infrared Imaging," 2012 IEEE International Conference on Electro/Information Technology, May 2012.

S. Bastas, G. Mirzaei, M. W. Majid, J. Ross, M. M. Jamali, J. Frizado, P. V. Gorsevski, V. Bingman, " A Novel Classification System for Flight Calls," The 2012 IEEE International Symposium on Circuits and Systems, Seoul, Korea, May 2012.

Golrokh Mirzaei, Mohammad Wadood Majid, Jeremy Ross, Mohsin M. Jamali, Joseph Frizado, Peter V. Gorsevski, Verner P. Bingman, "Feature Extraction and Classification of Bat Echolocation Calls," North American Symposium on Bat Research 2011, October 2011, Toronto, Canada

Golrokh Mirzaei, Mohammad Wadood Majid, Selin Bastas, Jeremy Ross, Mohsin M. Jamali, Peter V. Gorsevski, Joseph Frizado,Verner P. Bingman, "Acoustic Monitoring Techniques for Avian Detection and Classification," The Asilomar Conference on Signals, Systems, and Computers," November 2012.

Golrokh Mirzaei, Mohammad Wadood Majid, Jeremy Ross, Mohsin M. Jamali, Joseph Frizado, Peter V. Gorsevski, Verner P. Bingman, "Implementation of Ant Clustering Algorithm for IR Imagery in Wind Turbine Application", IEEE International Midwest symposium on Circuits and Systems, 2012.

Vamshi Gummalla, Nishatha Nagarajan, Jeremy Ross, Mohammad W. Majid, Mohsin. M. Jamali , Peter V. Gorsevski, Joseph P. Frizado, Verner P. Bingman, "A Radar Study of Nocturnal Bird Migration for Wind Turbine Siting Applications" 6th Annual Conference: Securing Ohio's Energy and Economic Future, Columbus, Ohio, April 2012

Golrokh Mirzaei, Selin A. Bastas, Jeremy Ross, Mohammad W. Majid, Mohsin. M. Jamali , Peter V. Gorsevski, Joseph P. Frizado, Verner P. Bingman, "Behavior Analysis of Birds/Bats Activity in the Vicinity of Wind Turbines" 6th Annual Conference: Securing Ohio's Energy and Economic Future, Columbus, Ohio, April 2012

Amin Jarrah, M. M. Jamali, Golrokh Mirzaei, Mohammad Wadood Majid, P. V. Gorsevski, J. Frizado, V.P.Bingman,"A Parallel Implementation for IR Video Processing on a GPU" 56th IEEE International Midwest symposium on Circuits and Systems, Columbus, Ohio, August 2013.

Priyadarsini Komatineni, Nishatha Nagarajan, Mohammad Wadood Majid, Golrokh Mirzaei, Jeremy Ross, Mohsin M. Jamali, Peter V. Gorsevski, Joseph Frizado, Verner P. Bingman, "Quantification of Bird Migration using Doppler Weather Surveillance Radars (NEXRAD)," Presented at the 2013 IEEE Radar Conference.

Golrokh Mirzaei, Mohsin M. Jamali, Peter V. Gorsevski, Joseph Frizado ,Verner P. Bingman, "Data Fusion of IR and Marine Radar Data," Asilomar Conference on Signals, Systems, and Computers," November 2013.

Lai Wei, Golrokh Mirzaei, Mohammad W. Majid, Mohsin M. Jamali, J. Ross, P. V. Gorsevski, V. P. Bingman, “Birds/Bats Movement Tracking with IR Camera for Wind Farm Applications, “The 2014 IEEE International Symposium on Circuits and Systems, Melbourne, Australia, June 2014. In-press.

**Theses and Dissertations**

Lee, Jin Woo. “Multilevel Decoupled Optimization of Wind Turbine Structures using Coefficients of Approximating Functions as Design Variables,” PhD Dissertation, 2014.

Jehan, Musarrat. “Bootstrapping and Separable Monte Carlo Simulation Methods Tailored for Efficient Assessment Failure Probability of Dynamic Systems,” PhD Dissertation, 2014.

Masoomi, Mohammad. “Numerical and Experimental Study of Offshore Wind Turbine Floating Platforms,” MS Thesis, 2014.

Rezaei, Ramin. “Experimental Study of Near Wake Flow of Upwind and Downwind Turbine Configurations,” MS Thesis, 2014.

Selin Bastas,”Development of Microphone Based Array DOA/Beamforming Based Sound Recognition System,” 2011

Priyadarsini Komatineni, “Quantification of Bird Migration Using Doppler Weather Surveillance Radars (NEXRAD),” May 2012

Lai Wei,” Birds/Bats Motion Tracking with Infrared Radiation Camera for Wind Farm Applications,” August 2012.

Nishatha Nagarajan,”Target Tracking Via Marine Radar,” August 2012.
Vamshi Gummala, “Monitoring of Bird Movement via Marine Radar in the Western Basin of Lake Erie,” November 2013

Addisu Dereje, “Wind Farm Site Suitability Analysis in Lake Erie Using Web-Based Participatory Gis (PGIS)”, January 2014

Sadat Hosseini, Seyyed Soheil, “Multiple Target Tracking via Marine Radar for bird strike and windfarm applications,” in progress

Golrokh Mirzaei, “Development of multi sensor system (Acoustic, IR and Radar) and data fusion for bat/bird monitoring for wind farm applications,” in-progress